Future Changes in Snowmelt-Driven Runoff Timing over the Western US

Sara A. Rauscher

Earth System Physics Section, The Abdus Salam International Centre for Theoretical Physics, Trieste, Italy.

Jeremy S. Pal

Department of Civil Engineering and Environmental Science, Seaver College of Science and Engineering, Loyola Marymount University, Los Angeles, California, USA

Noah S. Diffenbaugh

Purdue Climate Change Research Center and Department of Earth and Atmospheric Sciences, Purdue University, West Lafayette, Indiana, USA.

Michael M. Benedetti

Department of Geography and Geology, University of North Carolina Wilmington, Wilmington, North Carolina, USA.

We use a high-resolution nested climate model to investigate future changes in snowmelt-driven runoff (SDR) over the western US. Comparison of modeled and observed daily runoff data reveals that the regional model captures the present-day timing and trends of SDR. Results from an A2 scenario simulation indicate that increases in seasonal temperature of approximately 3° to 5° C resulting from increasing greenhouse gas concentrations could cause SDR to occur as much as two months earlier than present. These large changes result from an amplified snow-albedo feedback driven by the topographic complexity of the region, which is more accurately resolved in a high-resolution nested climate model. Earlier SDR could affect water storage in reservoirs and hydroelectric generation, with serious consequences for land use, agriculture, and water management in the American West.

1. Introduction

Runoff in mountainous regions is dominated by climatic variables such as temperature and precipitation, with runoff amount and timing varying with elevation [*Aguado et al.*, 1992]. The warming of 1°-2° C observed during the last half century over the western US has affected these climate-hydrology relationships [*Barnett et al.*, 2008]. Higher spring and winter temperatures appear to be causing decreasing trends in snow water equivalent (SWE) over the Pacific Northwest [*Mote*, 2003; *Mote et al.*, 2005] while shifting the timing of snowmelt-driven runoff (SDR) one to four weeks earlier in the year [*Cayan et al.*, 2001; *Stewart et al.*, 2005]. These changes are more pronounced at low and mid-elevations, while temperatures at higher elevations are still sufficiently low so that snowmelt timing has not changed to an observable degree [*McCabe and Clark*, 2005].

Temperatures are projected to rise by 3°-5° C over the western US by the end of this century as atmospheric greenhouse gas concentrations (GHGs) increase [*Christensen et al.*, 2007], resulting in further reductions in SWE, earlier spring SDR, and reduced water storage in the snowpack [e.g., *Hayhoe et al.*, 2004; *Leung et al.*, 2005]. Since SDR is the most predictable and reliable water resource in the western US [*Stewart et al.*, 2005], such changes could have substantial impacts, including on hydroelectric power generation, agriculture, and wildfire.

However, rigorous understanding of the potential impacts of climate change on SDR in the western US is complicated by the topographic complexity of the region. This topographic complexity is an important constraint on observed changes in SDR [*McCabe and Clark*, 2005], and it is likely to dictate the magnitude and spatial heterogeneity of

GHG-forced climate change [e.g., *Giorgi et al.*, 1997; *Leung and Ghan*, 1999]. Here we examine changes in SDR using daily fields from a high-resolution nested climate model. This approach allows us to both capture the fine-scale processes associated with topographic complexity and to quantify the temporal response of daily SDR.

2. Methods

We have performed two simulations using the ICTP Regional Climate Model (RegCM3) [*Pal et al.*, 2007] driven with initial and lateral boundary conditions from the NASA Finite Volume atmospheric GCM (FV-GCM)[*Atlas et al.*, 2005]; the model configurations are described in *Diffenbaugh et al.* [2005]. Annual time-varying concentrations of atmospheric carbon dioxide (CO2) for the RF run (1961-1989) are taken from *Schlesinger and Malyshev* [2001]. The future simulation (A2, 2071-2099) employs values from the A2 scenario described in the Special Report on Emissions Scenarios [*Nakicenovic et al.*, 2000] which assumes the global economy is regionally oriented with little convergence between the developed and developing worlds. Concern for the environment is fairly weak, resulting in high global population and GHG emissions relative to other scenarios. The mean global warming of 4°C is 0.5°C less than in the A1F1 scenario, but 1-2°C greater than in the A1B, A1T, B1 and B2 scenarios [*IPCC*, 2007].

Since the FV-GCM is not a coupled AOGCM, monthly time-varying sea surface temperatures (SSTs) from the Hadley Centre's observational data set (HadSST) [*Rayner et al.*, 2003] were prescribed for the RF run. Future SSTs were created by adding SST anomalies (A2-RF) calculated by HadCM3 A2 simulations to the HadSSTs. Snow accumulation and runoff in RegCM3 are handled by the Biosphere-Atmosphere Transfer Scheme (BATS)

[*Dickinson et al.*, 1993]. In BATS, runoff is a simple function of precipitation rate and soil water content relative to saturation. BATS divides runoff into base and surface flow components; the latter is large when the soil is saturated. Negative runoff may occur in BATS over irrigated areas. These few gridpoints (mostly in the Central Valley of California) are masked in the analysis.

To evaluate the model SDR timing with observations, daily discharge data from the U.S. Geological Survey Hydro-Climatic Data Network (HCDN) are used [*Slack and Landwehr*, 1992]. The HCDN dataset consists of high-quality stream gauge data collected for 1659 US sites from 1874-1988; stations that have been affected by urbanization, land cover changes, and measurement changes are excluded. For comparison with model output, data for water years (defined from Oct 1-Sep 30) 1962 to 1987 are selected for the conterminous US west of 105W. Only stations that are dominated by SDR (50% or more of the annual runoff occurs in April-July) and that have no missing data are included here [*Aguado et al.*, 1992], resulting in 141 stations (Figure 1:a). Most stations are at elevations between 100-2800 m and have basin drainage areas between 100-1000 km^2.

Previous studies of SDR timing changes using observed daily data employ two metrics: spring pulse onset and the center of mass of annual flow (CT) [e.g., *McCabe and Clark*, 2005; *Regonda et al.*, 2005]. Both metrics can be sensitive to "false starts" of the snowmelt season [*Stewart et al.*, 2005] as well as to both annual runoff and outliers [*Moore et al.*, 2007]. Therefore, following *Moore et al.* [2007], we calculated the Julian Day within the water year on which each percentile of that water year's annual flow occurred (DQF)[1]. To capture early, middle, and late-season flows, we show the 25th, 50th, and 75th DQFs.

These calculations are performed only for regions in which 50% or more of the annual runoff occurs in April-July.

3. Results

The RegCM3 RF run is able to capture the basic structure of SDR timing in the western US (Figure 1:a). There is particularly good agreement over eastern Oregon, western Idaho, western Montana, and the Sierra Nevadas, but in many areas the model lags the observations, especially over northern Nevada, southern Utah, and southern Colorado. These biases can be attributed to a combination of factors which may be operating differently in different regions. First, the RF run displays a negative surface air temperature bias (compared to observations) and a positive precipitation bias during winter and spring[2], which will tend to increase model snowcover and delay melting. This cold bias occurs in other RegCM3 simulations [*Pal et al.*, 2007]. Variable success in modeling soil moisture may also affect SDR timing. In BATS, moisture storage capacity is determined as a function of soil texture. This is realistic across much of the Mountain West, where thick glacial deposits fill most river basins, but less so over the Southern Rockies where soil cover is thin and rivers are less dependent on antecedent conditions. To further validate the model performance, the linear trend for the 50th DQF was calculated for the RF run and the observations (Figure 1:b). Both show a trend towards earlier SDR timing, particularly over the Northwest and the Sierra Nevada. Over Colorado and northern New Mexico, there is mix of responses with both later and earlier SDR.

For most of the western US, SDR is projected to occur earlier in the A2 simulation than in the RF simulation (Figure 1:c-e). For the 25th DQF (the Julian Day on which 25%

of that year's flow has occurred, analogous to the spring pulse onset of SDR), the largest changes of 70 days or more are projected to occur in the Sierra Nevada of California, the Cascades of Washington, and in the Bitterroot Range of northeastern Idaho and western Montana. Earlier timing of 20-40 days are projected in the eastern Rocky Mountains in Colorado, the Wasatch Range in northern Utah, and the Sangre de Cristo in southern Colorado and northern New Mexico. With the exception of central California, the greatest projected changes in SDR occur **a**t elevations between 1200-1800 m^3. In addition, the changes in SDR decrease progressively from the 25th to the 75th DQF (Figure 1:c-e), resulting in both a widening of the annual hydrograph and a leftward (earlier) shift on the time axis.

4. Discussion

The response of SDR to climate changes driven by elevated GHGs over the RegCM3 domain is dominated by increases in winter temperatures (up to 5° C) and associated reductions in snow cover (Figure 2:g,c). More specifically, the temperature increases reduce the amount of land covered by snow and hence the surface albedo (reflectivity). This results in an increase in the amount of surface absorbed solar radiation (Figure 2:d) and further amplifies the surface warming, resulting in additional melting and a positive feedback (known as the snow-albedo feedback). The temperature change is much greater in RegCM3 (Figure 2:g) compared to FV-GCM (Figure 2:f) in association with decreases in snow cover and an increase in net surface shortwave radiation. The pattern and magnitude of these changes are regulated primarily by topography. For example, large increases in temperature over central and eastern Washington State and the high elevations of Cal-

ifornia correspond to large decreases in accumulated snow. These same regions indicate the largest increases in net surface shortwave radiation.

This enhanced temperature response does not occur in FV-GCM nor most other GCM climate change simulations, which have a smooth representation of topography and artificially low elevations in the western US. For example, using a GCM forced by an IS92a-like scenario that results in CO2 levels at 710 ppmv by 2100 [*Dai et al.*, 2001], *Stewart et al.* [2004] found changes in CT of only up to 35 days for the Northwest and Sierra Nevada. Using the same GCM simulations to drive a hydrologic model, *Christensen et al.* [2004] noted earlier runoff timing of only about 1 month for rivers in the Colorado Basin. More recent results using the VIC model driven by CMIP3 model output for the A2 scenario indicate earlier CTs of only 23 to 36 days for basins in the Sierra Nevada [*Maurer*, 2007]. These changes were attributed to an increase in surface air temperature of approximately 3-3.7° C, which is similar to the FV-GCM temperature change. Therefore, the amplified SDR response (in many regions a factor of 2 greater than previous studies using GCM output) reported in RegCM3 appears to be due to the enhanced temperature response of the high-resolution model associated with the topography-dependent snow-albedo feedback.

Precipitation changes do occur in our A2 simulation; precipitation increases over the Northwest and decreases over northern California and the Southwest (Figure 2:a), a common feature of climate change simulations that is usually attributed to a northward shift of the mid-latitude winter storm track [*Yin*, 2005]. In the A2 simulation there is anomalous cyclonic flow over the Southwest and increased upslope flow over western mountain ranges (Figure 2:e). Combined with higher atmospheric moisture content, these changes

lead to increased precipitation and a weakening of the rainshadow effect over Colorado and Wyoming while contributing to drying over California [*Diffenbaugh et al.*, 2005]. However, runoff increases more than precipitation (Figure 2:a-b), again indicating the effect of higher temperatures and earlier snowmelt.

Further, these circulation changes and higher atmospheric moisture content do not increase accumulated snow since late winter and spring temperatures are higher and there are fewer annual days below freezing (Figure 2:g,h). Thus, temperature seems to be the dominant factor in determining changes in runoff, consistent with observations [*Dettinger and Cayan*, 1995]. Also, despite the increase in precipitation over the Northwest, accumulated snow decreases in the A2 simulation even at the highest elevations of the Cascades, in agreement with GCM simulations [*Kim et al.*, 2002; *Leung et al.*, 2005; *Hayhoe et al.*, 2004]. Moreover, our projected changes in SDR timing are consistent with the observed spatial pattern; larger changes occur over the Northwest [*Regonda et al.*, 2005] and smaller changes are found over interior mountain ranges such as the Rockies [e.g., *Hamlet et al.*, 2005].

One important caveat is that although our experimental design accounts for changes in mean SST (as described in Section 2), it assumes little change in interannual SST variability between the RF and A2 periods. Some hydroclimatic trends over the western US have been partly linked to changes in ENSO and the PDO [e.g., *Cayan et al.*, 1999]. While future changes in those modes of variability could create a different precipitation regime [*Moore et al.*, 2007], the dominance of temperature effects suggests that the early SDR timing trend identified here is unlikely to be reversed.

5. Conclusions

We have used a nested high-resolution climate model to investigate future changes in SDR over the western US. A comparison of modeled SDR with HCDN data reveals that RegCM3 captures the present-day timing of SDR as well as observed trends. Results from a late-21st century simulation (A2 scenario) indicate that increases in temperature, forced by increasing GHGs, could cause early-season SDR to occur as much as two months earlier than present, particularly in the Northwest. Earlier SDR timing of at least 15 days in early-, middle-, and late-season flow is projected for almost all mountainous areas where runoff is snowmelt-driven. These large changes result from an amplified snow-albedo feedback associated with the topographic complexity of the region.

Reduced snowpack and early SDR are likely to result in substantial modifications to the hydrologic cycle, including increased winter and spring flooding; changes in lake, stream, and wetland ecology; and reduced riverflow and natural (snow and soil) storage [*Cayan et al.*, 2007]. For example, lower summer soil moisture could increase forest fire frequency and intensity [*Westerling et al.*, 2006]. Moreover, water supplies for sectors including (but not limited to) agriculture [e.g., *Purkey et al.*, 2008], energy [e.g., *Markoff and Cullen*, 2008; *Vicuna et al.*, 2008], and recreational use [e.g., *Hayhoe et al.*, 2004] could be severely affected, necessitating additional reservoirs and/or extended reservoir capacity. These changes to the hydrological cycle are likely to result in numerous societal and economic impacts that will pose serious challenges for water and land use management in the future.

Acknowledgments. We thank two anonymous reviewers for very useful comments.

Notes

1. Auxiliary Materials: Figure S1

2. Auxiliary Materials: Figure S2

3. Auxiliary materials, Figure S3

References

Aguado, E., D. Cayan, L. Riddle, and M. Roos (1992), Climatic fluctuations and the timing of West Coast streamflow, *J. Climate*, *5*, 1468–1483.

Atlas, R., et al. (2005), Hurricane forecasting with the high-resolution NASA finite volume general circulation model, *Geophys. Res. Lett.*, *32*, L03,807, doi:10.1029/2004GL021513.

Barnett, T. P., et al. (2008), Human-induced changes in the hydrology of the western United States, *Science*, *319*, 1080–1083, doi:10.1126/science.1152538.

Cayan, D. R., K. T. Redmond, and L. G. Riddle (1999), ENSO and hydrologic extremes in the western United States, *J. Climate*, *12*, 2881–2893.

Cayan, D. R., S. A. Kammerdiener, M. D. Dettinger, J. M. Caprio, and D. H. Peterson (2001), Changes in the onset of spring in the western United States, *Bull. Am. Meteorol. Soc.*, *82*, 399–416.

Cayan, D. R. A. L. Luers, G. Franco, M. Hanemann, B. Croes, and E. Vine (2007), Overview of the California climate change scenarios project, *Clim. Change*, *72*, S1–S6.

Christensen, J. H., et al. (2007), Regional climate projections, in *Climate Change 2007: The Physical Science Basis. Contribution of Working Group I to the Fourth Assessment Report of the Intergovernmental Panel on Climate Change*, edited by S. Solomon,

D. Qin, M. Manning, Z. Chen, M. Marquis, K. Averyt, M. Tignor, and H. Miller, chap. 11, pp. 235–336, Cambridge University Press, New York.

Christensen, N. S., A. W. Wood, N. Voisin, D. P. Lettenmaier, and R. N. Palmer (2004), The effects of climate change on the hydrology and water resources of the Colorado River basin, *Clim. Change*, *62*, 337–363.

Coppola, E., and F. Giorgi (2005), Climate change in tropical regions from high-resolution time-slice AGCM experiments, *Quart. J. Roy. Meteor. Soc.*, *131*, 3123–3145.

Dai, A., T. M. L. Wigley, B. A. Boville, J. T. Kiehl, and L. E. Buja (2001), Climates of the twentieth and twenty-first centuries simulated by the NCAR Climate System Model, *J. Climate*, *14*, 485–519.

Dettinger, M. D., and D. R. Cayan (1995), Large-scale atmospheric forcing of recent trends toward early snowmelt runoff in California, *J. Climate*, *8*, 606–623.

Dickinson, R. E., A. Henderson-Sellers, and P. J. Kennedy (1993), Biosphere-atmosphere transfer scheme (BATS) version 1E as coupled to the NCAR Community Climate Model, *NCAR Tech. Note NCAR/TN-387+STR*, National Center for Atmospheric Research, National Center for Atmospheric Research, Boulder, CO 80307.

Diffenbaugh, N. S., J. S. Pal, R. J. Trapp, and F. Giorgi (2005), Fine-scale processes regulate the response of extreme events to global climate change, *Proc. Nat. Acad. Sci. USA*, *102*, 15,774–15,778, doi:10.1073/pnas.0506042102.

Giorgi, F., J. W. Hurrell, M. R. Marinucci, and M. Beniston (1997), Elevation dependency of the surface climate change signal: A model study, *J. Climate*, *10*, 288–296.

Hamlet, A. F., P. W. Mote, M. P. Clark, and D. P. Lettenmaier (2005), Effects of temperature and precipitation variability on snowpack trends in the western United States, *J. Climate*, *18*, 4545–4561.

Hayhoe, K., et al. (2004), Emissions pathways, climate change, and impacts on California, *Proc. Nat. Acad. Sci. USA*, *101*, 12,422–12,427.

Intergovernmental Panel on Climate Change (IPCC) (2007), *Climate Change: The Physical Science Basis. Contribution of Working Group I to the Fourth Assessment Report of the IPCC*, in press. (Available online from http://www.ipcc.ch)

Kim, J., T.-K. Kim, R. W. Arritt, and N. L. Miller (2002), Impacts of increased atmospheric CO2 on the hydroclimate of the western United States, *J. Climate*, *15*, 1926–1942.

Leung, L. R., and S. J. Ghan (1999), Pacific Northwest climate sensitivity simulated by a regional climate model driven by a GCM. Part II: Simulations, *J. Climate*, *12*, 2031–2053.

Leung, L. Y. R., Y. Qian, X. Bian, W. M. Washington, J. Han, and J. Roads (2005), Mid-century ensemble regional climate change scenarios for the western United States, *Clim. Change*, *62*, 75–113.

Markoff, M. S., and A. C. Cullen (2008), Impact of climate change on Pacific Northwest hydropower, *Clim. Change*, *87*, 451–469.

Maurer, E. P. (2007), Uncertainty in hydrologic impacts of climate change in the Sierra Nevada, California, under two emissions scenarios, *Clim. Change*, *82*, 309–325.

McCabe, G., and M. Clark (2005), Trends and variability in snowmelt runoff in the western United States, *J. Hydrometeor.*, *6*, 476–482.

Moore, J. N., J. T. Harper, and M. C. Greenwood (2007), Significance of trends toward earlier snowmelt runoff, Columbia and Missouri Basin headwaters, western United States, *Geophys. Res. Lett.*, *34*, L16,402, doi:10.1029/2007GL031022.

Mote, P. W. (2003), Trends in snow water equivalent in the Pacific Northwest and their climatic causes, *Geophys. Res. Lett.*, *30*, 1601, doi:doi:10.1029/2003GL017258.

Mote, P. W., A. F. Hamlet, M. P. Clark, and D. P. Lettenmaier (2005), Declining mountain snowpack in western North America, *Bull. Am. Meteorol. Soc.*, *86*, 39–49.

Nakicenovic, N., et al. (2000), *IPCC Special Report on Emissions Scenarios*, 599 pp., Cambridge Univ. Press, New York.

Pal, J. S., et al. (2007), Regional climate modeling for the developing world: The ICTP RegCM3 and RegCNET, *Bull. Am. Meteorol. Soc.*, *88*, 1395–1409.

Payne, J. T., A. W. Wood, A. F. Hamlet, R. N. Palmer, and D. P. Lettenmaier (2004), Mitigating the effects of climate change on the water resources of the Columbia River basin, *Clim. Change*, *62*, 233–256.

Purkey, D. R., B. Joyce, S. Vicuna, M. W. Hanemann, L. L. Dale, D. Yates, and J. A. Dracup (2008), Robust analysis of future climate change impacts on water for agriculture and other sectors: a case study in the Sacramento Valley, *Clim. Change*, *87*, S109–S122.

Rayner, N. A., D. E. Parker, E. B. Horton, C. K. Folland, L. V. Alexander, D. P. Rowell, E. C. Kent, and A. Kaplan (2003), Global analyses of sea surface temperature, sea ice,

and night marine air temperature since the late nineteenth century, *J. Geophys. Res.*, *108*, 4407, doi:10.1029/2002JD002670.

Regonda, S. K., B. Rajagopalan, M. Clark, and J. Pitlick (2005), Seasonal cycle shifts in hydroclimatology over the western United States, *J. Climate*, *18*, 372–384.

Schlesinger, M. E., and S. Malyshev (2001), Changes in near-surface temperature and sea level for the Post-SRES CO2-stabilization scenarios, *Integrated Assessment*, *2*, 95–110.

Slack, J. R., and J. M. Landwehr (1992), Hydro-climatic data network (HCDN): A U.S. geological survey streamflow data set for the United States for the study of climatic variations, 1874-1988, *Open-File Report 92-129*, U.S. Geological Survey, Reston, Virginia.

Stewart, I. T., D. R. Cayan, and M. D. Dettinger (2004), Changes in snowmelt runoff timing in western North America under a 'Business as Usual' climate change scenario, *Clim. Change*, *63*, 217–332.

Stewart, I. T., D. R. Cayan, and M. D. Dettinger (2005), Changes toward earlier streamflow timing across western North America, *J. Climate*, *18*, 1136–1155.

Vicuna, S., R. Leonardson, M. W. Hanemann, L. L. Dale, and J. A. Dracup (2008), Climate change impacts on high elevation hydropower generation in Californias Sierra Nevada: A case study in the Upper American River, *Clim. Change*, *87*, S123S137.

Westerling, A. L., H. G. Hidalgo, D. R. Cayan, and T. W. Swetnam (2006), Warming and earlier spring increase western U.S. forest wildfire activity, *Science*, *313*, 940–943.

Yin, J. H. (2005), A consistent poleward shift of the storm tracks in simulations of 21st century climate, *Geophys. Res. Lett.*, *32*, L18,701, doi:10.1029/2005GL023684.

Figure 1. Average Julian Day of the 50th DQF for RegCM3 reference simulation (shaded grid cells) and U.S. Geological Survey Hydro-Climatic Data Network (HCDN) stations (filled circles) for 1962-1987 (a), Linear trend (days per decade) in the 50th DQF for 1962-1987; positive values indicate a trend toward earlier snowmelt-driven runoff through the 26 year period (b), and differences between the future and reference simulations for the 25th (c), 50th (d), and 75th (e) DQF (date of quarterly flow) (days). For c-e, positive values indicate snowmelt-driven runoff occurs earlier in the A2 scenario simulation. Only differences significant at the 95% level using a two-tailed student t-test are shown.

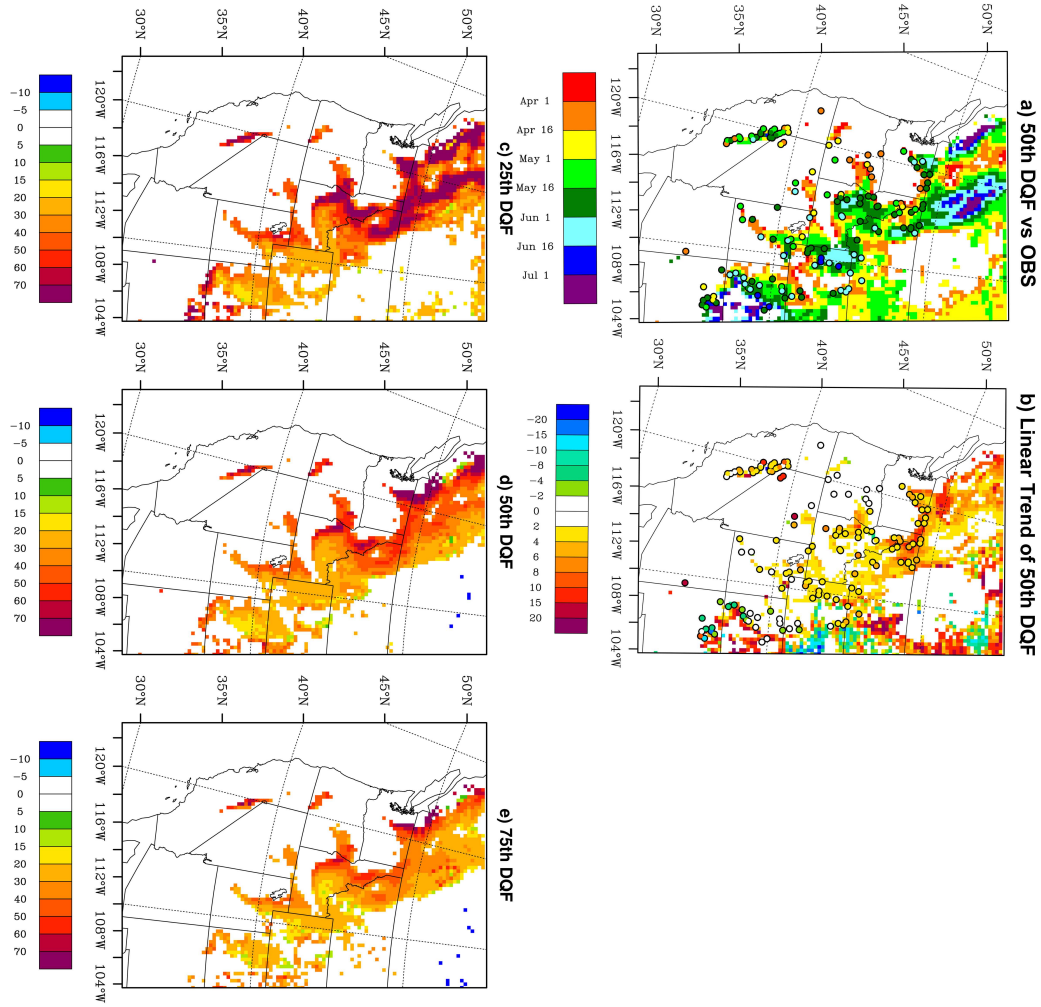

Figure 2. Average winter (JFM) (except panel h) RegCM3 (except panel f) A2-RF differences for a) precipitation (mm day^{-1}) b) runoff (mm day^{-1}) c) snow accumulation (mm snow water equivalent) d) net surface shortwave radiation flux (W m^{-2}) e) 700 hPa geopotential heights (m) and wind vectors (m s^{-1}) f) FV-GCM surface temperature change (° C) g) surface temperature change (° C) h) annual change in number of days below freezing

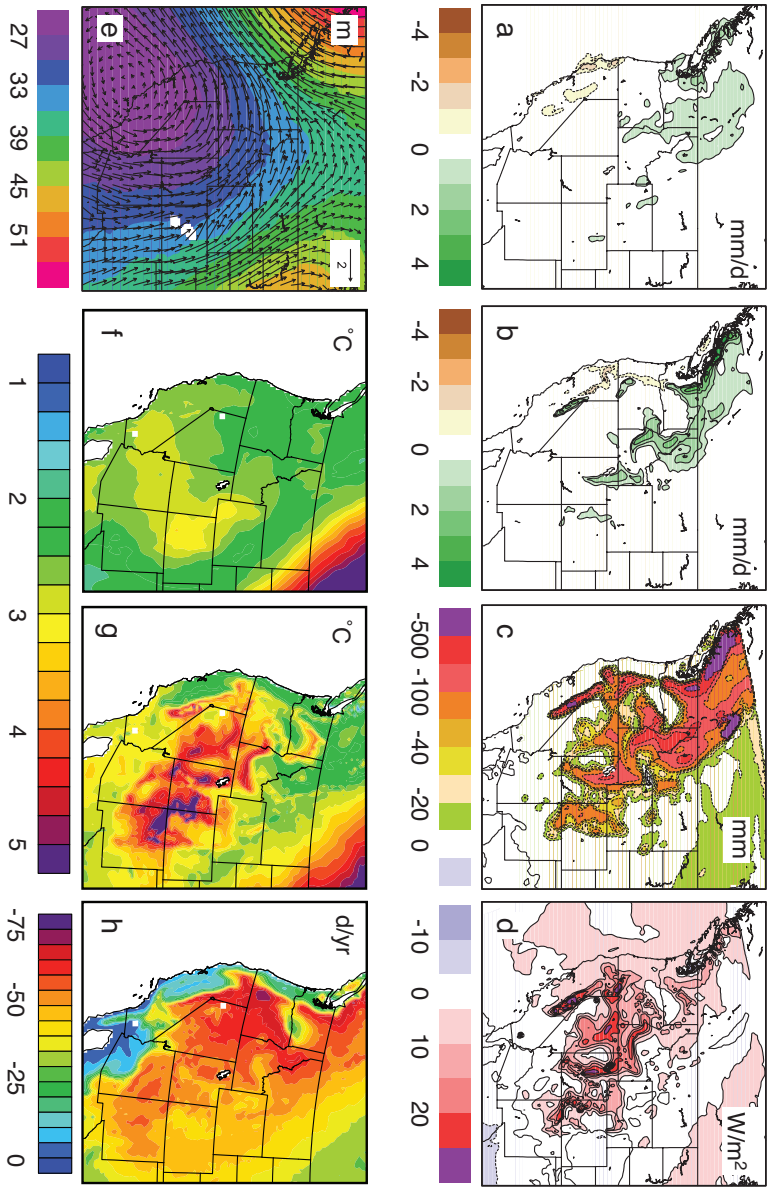

Figure S1. Daily runoff (solid) and accumulated runoff (dashed) (cf/s) during water year 1964 for Boise River, Idaho (HCDN station 13185000). The 25th, 50th, and 75th DQF are marked by vertical red lines.

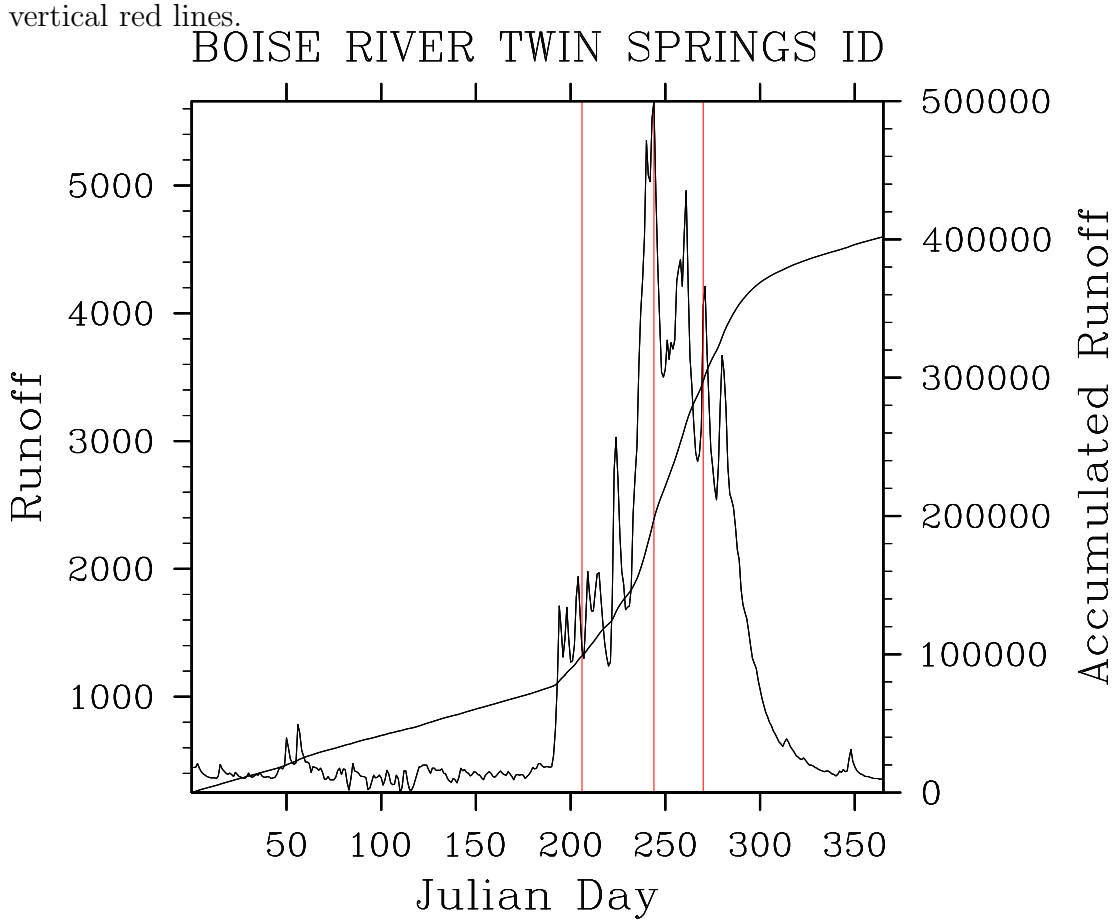

Figure S2. Average surface air temperature (degrees C, left two columns) for JFM (a-c) and OND (d-f) and precipitation (mm/day, right two columns) for JFM (g-i) and OND (j-l) for Climate Research Unit (CRU) observations [Mitchell and Jones 2005] (top), RegCM3 (middle), and FV-GCM (bottom). The CRU observations are a gridded 0.5 degree monthly precipitation and temperature dataset (land-only) derived from station observations.

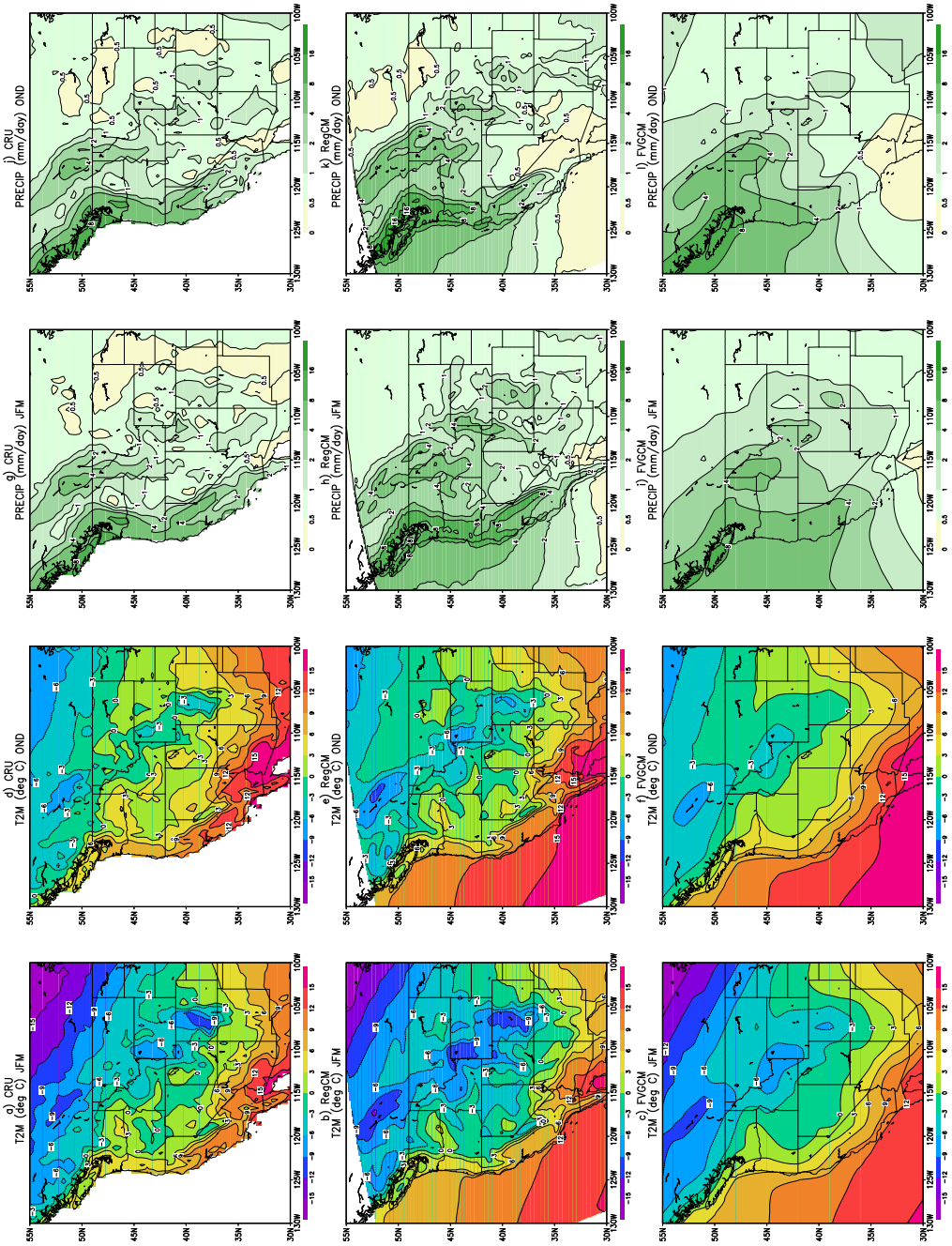

Figure S3. Change (A2-RF) in runoff date vs. elevation for the a) 25th DQF b) 50th DQF c) 75th DQF for each of the model gridpoints and change in snowmelt-driven runoff date of the 25th DQF vs. change in March-June (spring) ground temperature (degrees C) for elevations d) 500-1500 m e) 1500-2500 m and f) greater than 2500 m.